International Institute for
Applied Systems Analysis
Schlossplatz 1
A-2361 Laxenburg, Austria

Tel: +43 2236 807 342
Fax: +43 2236 71313
E-mail: publications@iiasa.ac.at
Web: www.iiasa.ac.at

Interim Report **IR-02-046**

Looking Behind the Kyoto Protocol: Can Integral Transforms Provide Help in Dealing with the Verification Issue?

Volodymyr Dachuk (dachuk@dndiii.lviv.ua)

Approved by

Sten Nilsson
Deputy Director and Leader, Forestry Project

July 2003

Contents

Abstract

The verification of net greenhouse gas emission changes, as required under the Kyoto Protocol, is not yet fully understood. This report reflects the attempt to explore the usefulness of Laplace integral transform techniques to grasp the dynamics of emissions and emission uncertainties in order to understand verification characteristics of different systems emitting greenhouse gases. The study is based on the Verification Time Concept proposed by IIASA's Forestry Project. The Laplace integral transform is applied to describe the dynamics of emissions and uncertainties.

Acknowledgments

I would like to thank Matthias Jonas, who supervised this work, and Anatoly Shvidenko both working in IIASA's Forestry (FOR) Project for the many discussions and their comments. I am also indebted to Shari Jandl for her valuable editorial assistance, and all the Forestry team for their support. It is my pleasure to thank the YSSP coordinator, Margaret Traber, and all IIASA staff who did everything possible to make my stay at IIASA pleasurable. Appreciation goes to the Swedish NMO — The Swedish Research Council for Environment, Agricultural Sciences and Spatial Planning (FORMAS) for their generous financial support.

About the Author

Volodymyr Dachuk is a senior research scientist at the Department of Information Technologies for Modeling and Prognosis of Complex Processes and Phenomena at the State Research Institute of Information Infrastructure in Lviv, Ukraine. In the summer of 2001, Volodymyr Dachuk was a participant in IIASA's Young Scientists Summer Program (YSSP) assigned to the Forestry (FOR) Project. Volodymyr Dachuk was involved in FOR's research focusing on greenhouse gases and the Kyoto negotiations and specifically he dealt with IIASA's higher-order verification time concept.

Looking Behind the Kyoto Protocol: Can Integral Transforms Provide Help in Dealing with the Verification Issue?

Volodymyr Dachuk

1 Introduction

According to the United Nations Framework Convention on Climate Change (UNFCCC), the atmospheric concentration of greenhouse gases (GHG) should ultimately be stabilized at a level that would prevent dangerous anthropogenic interference with the climate system. To attain this objective, the emissions of greenhouse gases should be limited considerably. In Kyoto in 1997, the parties of the convention agreed on emissions reductions in industrialized countries (UNFCCC, 1998). The Kyoto Protocol to the UNFCCC obligates the Annex I countries to reduce their greenhouse gas emissions by the first commitment period (2008–2012) relatively to their base year (1990 for most countries). However, the Protocol leaves still unresolved the question of verifying the changes of GHG emissions, which in most cases are reported to be less than the corresponding uncertainties in emissions data.

Current scientific understanding of the various human-induced processes, which lead to emissions and removals of GHGs to and from the atmosphere, is incomplete. In some cases, where substantial measurement data exist and have been thoroughly analyzed, this understanding provides a basis for accurate calculation of global and national emissions. In many cases, however, data and analysis have not attained this state. This affects the uncertainty inherent in the various components of the default methods, as well as the estimates using other methodologies. Therefore, the verification-uncertainty issue in the context of the Kyoto Protocol still experiences serious methodological difficulties.

Even without considering the uncertainties that underlie the emission data, verification under the Kyoto Protocol is not clear because it does not take into account the dynamics of changes in emissions. An example (Figure 1) illustrates this. Let us consider the behavior of a system (e.g., an Annex I country) emitting GHGs between two points in time t_1 (the base year) and t_2 (the commitment year). According to the Protocol, these three strategies are conceivable. However, following strategy 2, the country emits in total fewer GHGs than under strategy 1, because the total amount of carbon emitted during the period of time between points t_1 and t_2 is proportional to the area of curvilinear trapezoid bounded by emission curve $s(t)$ and the time axis. The country can choose strategy 1 as the most profitable for itself, because it permits the

accumulation of most products of some kind (energy, feedstock, goods, etc.), and at the same time satisfies the conditions of the Kyoto Protocol. But there is strategy 3, under which the country does not satisfy the conditions of the Kyoto Protocol, although total emissions are less than under strategies 1 or 2. The example reveals the insufficiency of considering only two points in time t_1 and t_2 for verification. The ideal point in time for verification would be the case when each point in time between t_1 and t_2 is taken into account, or alternatively, taking into account dynamical moments of emissions in order to reproduce the behavior of emission function $s(t)$ on the time segment $[t_1, t_2]$. So, the dynamical moments of emissions (or the total amount of carbon emitted) should be considered under the Kyoto Protocol. At present, the Kyoto concept for verification is static: only two points in time (final and base years) are considered, and the dynamics of emissions between these points are not taken into account. Taking the uncertainties into account complicates the process of verification.

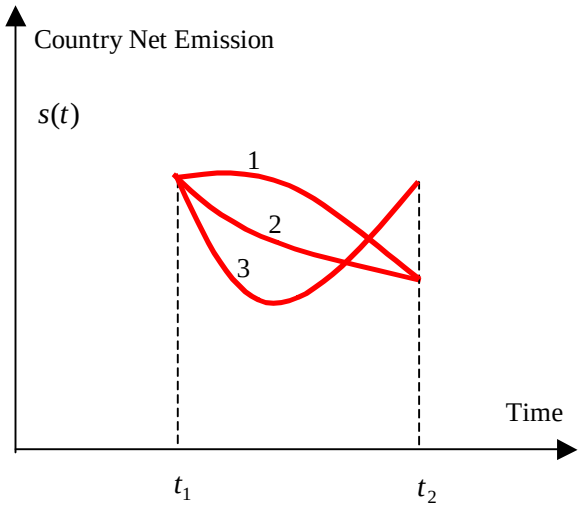

Figure 1: Conceivable strategies of an Annex I country fulfilling the Kyoto Protocol.

Countries differ from each other in their potential for reducing emissions and in the economic consequences of emission limitations. This is due to their different characteristic conditions and available resources, energy systems and economies, including historical development and wealth. This difference is directly connected with countries' abilities to fulfill their Kyoto obligations. Considering uncertainties in reported national emissions data make the task of verifying emission changes intricate insofar as verifying these changes demands a sound and robust strategy, which is not available now.

This paper aims at developing the basis for accounting GHG emissions in consideration of verification and uncertainty. The main focus of the approach presented here is to uncover the emission and uncertainty dynamics that is characteristic for a given GHG emitting system with the help of the Laplace integral transform. The Laplace integral transform is applied to describing the dynamics of emissions and the underlying uncertainties. Traditionally this transform is used for solving difference and differential equations, i.e., finding the unknown functions from such equations. Here, in a certain

sense the inverse task is posed, that is to determine the dynamical parameters of systems with the help of the Laplace integral transform.

The results of Jonas *et al*. (1999a, b) and Gusti and Jęda (2002), who studied the verifiability of carbon accounts under the Kyoto Protocol by acknowledging the uncertainty underlying such accounts, provide the basis for this study. The authors evaluated questions related to the methods used for verifying carbon accounts and the effect of different provisions on the feasibility of implementing the Protocol by developing and applying the concept of "verification time". This is the minimal time required to verify changes in GHG emissions. It links the dynamics of carbon emissions with the dynamics of the underlying uncertainties. In contrast to these earlier studies, where the verification time concept is considered in light of emission's and uncertainties' dynamical moments of the first and second order, this study investigates the ability of Laplace integral transforms to grasp dynamical characteristics of systems emitting greenhouse gases.

The verification time concept dates back to the IIASA FOR Project's studies on full carbon accounts for Russia and Austria (Nilsson *et al*., 2000; Jonas and Nilsson, 2001). The concept gave rise to a number of urgent issues and corresponding problems, which were discussed by the authors in a number of IIASA reports (Jonas *et al*., 1999a, b, 2000; Obersteiner *et al*., 2000a, b, c; Jonas and Nilsson, 2001; Gusti and Jęda, 2002).

2 Methodology

This section introduces the IIASA/FOR's verification time concept and the application of the Laplace integral transform to verification time calculations.

2.1 Verification Time Concept

The method for determining the verification time for dynamical systems emitting GHGs was proposed by IIASA's FOR Project. It is based on a reasonable standard condition for verification (Jonas *et al.*, 1999a). This condition states (Figure 2) that the absolute change in a country's net carbon emissions (emission signal) at time t_2 with reference to time t_1 ($t_1 < t_2$) is greater than the uncertainty in the reported net carbon emissions at time t_2.

If we have the emission signal $|s(t) - s(t-\tau)|$ and the level of uncertainties $\varepsilon(t)$, then the signal can be verifiable only when it outstrips the level of uncertainties (Jonas *et al*, 1999a):

$$|s(t) - s(t-\tau)| \geq \varepsilon(t). \qquad (1)$$

Inequality (1) is the mathematical formulation of the verification time concept. One can assume that functions describing emission $s(t)$ and uncertainty $\varepsilon(t)$ are smooth enough so that they can be represented by polynomials in the independent variable t. If we

decompose the emission and uncertainty functions $s(t)$ and $\varepsilon(t)$ in t_1 with the help of a Taylor series and limit the emission function $s(t)$ to the *n*-th order and the uncertainty function $\varepsilon(t)$ to the *m*-th order, one can calculate the verification time (VT) $\tau = t_2 - t_1$.

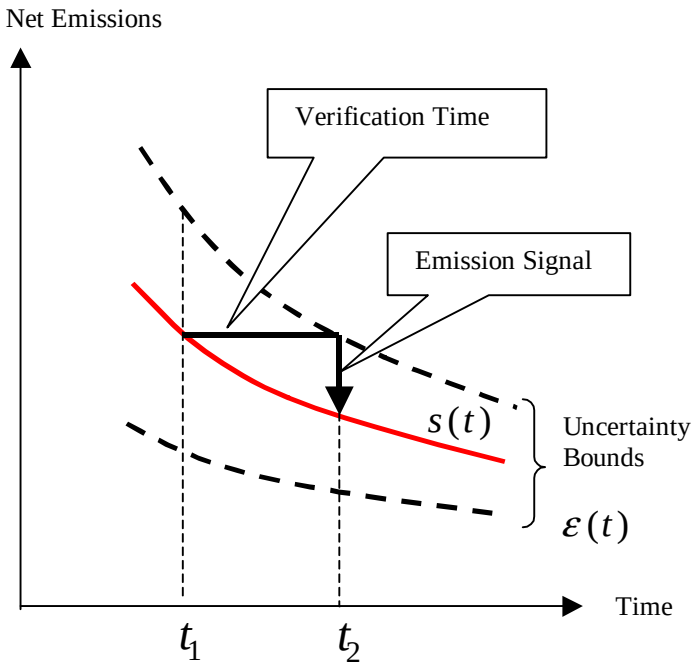

Figure 2: The Verification Time Concept as introduced by Jonas *et al*. (1999a).

Gusti and Jęda (2002) have investigated the case of representing emission signals (reflecting the burning of fossil fuels, the production of cement, and the flaring of gas) and their uncertainties by first and second-order polynomials. The authors considered only CO_2 emissions and used in their estimations the UNFCCC database (UNFCCC, 2000) and global, regional, and national CO_2 emissions data by Marland *et al*. (1999), where uncertainty of global emissions is more than 10%, uncertainties in national estimates for different sectors are in the range of 10–25% (IPCC/OECD/IEA, 1997), and the overall uncertainty in emission estimates reported to the IPCC are about 20% (IPCC, 2000). Gusti and Jęda (2002) have calculated verification times for all Annex I countries. Their study shows that for Annex I countries the verification time is in the range of a few years to decades. So, according to this study, most Annex I countries will most likely be able to verify their national emission changes from fossil fuels burning, cement production and gas flaring by 2010. But taking into consideration the emissions from sectors of agriculture and land use change and forestry, where uncertainties in emission data are significant, may complicate verification (the verification time increases in general).

To determine verification time τ, let us continue from inequality (1). In the case of a second-order emission signal and a first-order uncertainty, we obtain the equation:

$$\left| \frac{ds(t_1)}{dt}\tau + \frac{1}{2}\frac{d^2 s(t_1)}{dt^2}\tau^2 \right| = \varepsilon(t_1) + \frac{d\varepsilon(t_1)}{dt}\tau \,. \qquad (2)$$

After obtaining a set of solutions of the kind in equation (2), we chose such τ that are real, greater than zero, and are the smallest among the valid ones. Additionally, there are no solutions if uncertainty is increasing faster than emissions are changing (Gusti and Jeda, 2002).

As demonstrated by Gusti and Jęda (2002), the non-linearity of equation (2) leads to interesting surprises like, e.g., a "jumping" VT depending on the dynamics of uncertainty (Figure 3) or other parameters of the equation. This results from non-uniqueness of the roots of equation (2): the verification time is given by the minimal solution among them. The graphical solution of equation (2) is presented in Figure 4, which also exhibits the "jumpy" nature of the VT.

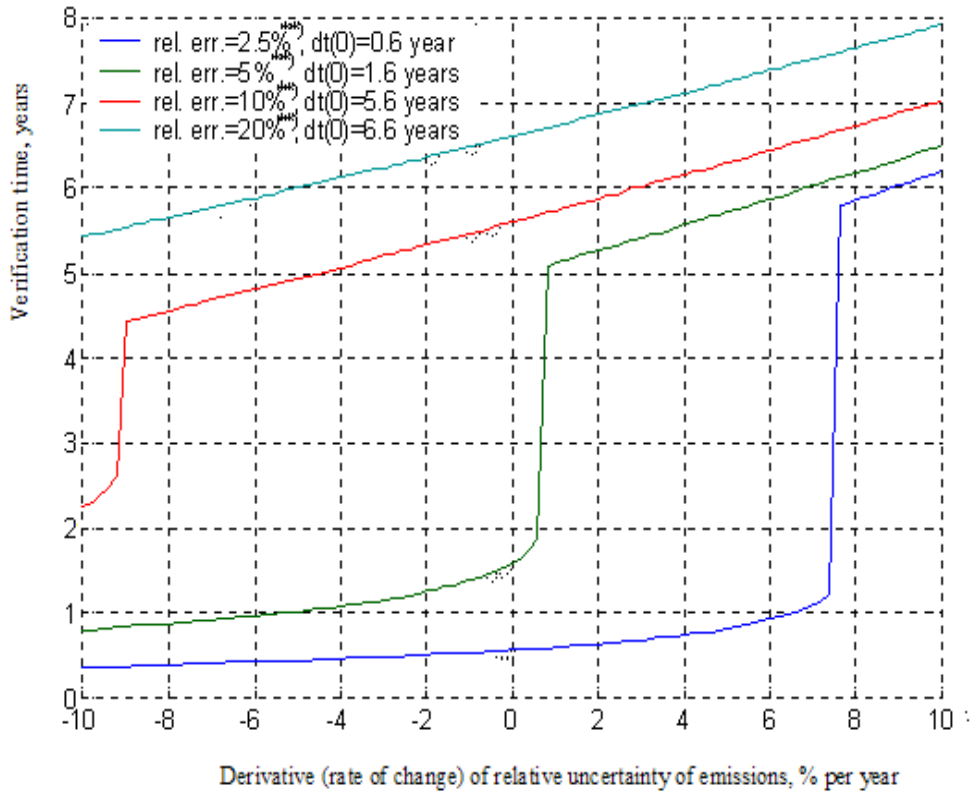

Figure 3: Illustration of the "jumpy" VT character depending on the dynamics of uncertainty, here for the fossil fuel emissions including cement production (second-order approach) from the Russian Federation (Gusti and Jęda, 2002).

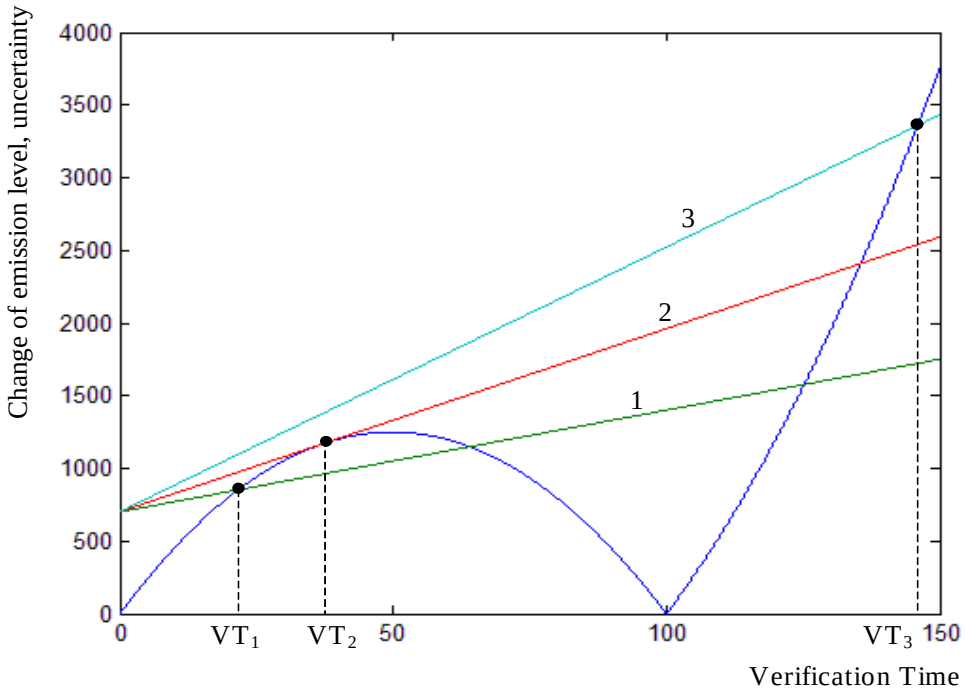

Figure 4: Graphical solution of equation (2). The straight lines (1, 2 and 3) represent the right side of the equation for various uncertainty growth rates. The curve represents the left side of the equation. It becomes obvious that a little change in the derivative of uncertainty (slope of the straight line) may cause a considerable change in the verification time ($VT_1 < VT_2 << VT_3$).

As one can conclude after analyzing Figure 4, the polynomial expansion for the emission (and uncertainty) function to higher (more than 2) order may lead to more jumps of verification time (for example, for third-order dynamics, we may expect two jumps, and so on).

2.2 The Basics of Operational Calculus and Integral Transforms

The purpose of this section is to introduce the basic techniques of operational calculus and to make use of them for our VT calculations. The particular transforms discussed here are the Laplace, Fourier and *z*-transforms, but the main attention is paid to the Laplace integral transform. Another objective of this section is to acquaint the reader with the idea of implementing the Laplace integral transform for solving and analyzing verification inequality (1), which is a difference inequality and can be solved (analyzed) more easily with the help of this transform.

2.2.1 Operational methods

The concept of the operational method is based on a functional transformation such as those provided by the Fourier and Laplace integrals. One can think, e.g., of the act of

differentiation as a transformation, where operator **D** transforms a function $s(t)$ into a function $s'(t)$. That is,

$$\mathbf{D}\{s(t)\} = s'(t). \tag{3}$$

The function $s'(t)$ is the transform of $s(t)$ under the transformation. For example, we could view the function $2t$ as a transform of t^2. In a similar fashion, the act of integration can also be viewed as a transformation. The operation:

$$\mathbf{I}\{s(t)\} = \int_0^x s(t)\,dt = g(x) \tag{4}$$

transforms the function $s(t)$ to the functional $g(x)$. Even the operator that multiplies all the functions by the same constant can be viewed as a transformation.

The integral transform of function $s(t)$ is defined as transformation:

$$\mathbf{F}\{s(t)\} = \int_a^b s(t)K(t, p)dt = S(p). \tag{5}$$

The kind of integral transform and its character depend on the option of limits on integral a and b, and also on function $K(t, p)$ of variable t and parameter p. $K(t, p)$ is called the kernel of integral transform (5), and $S(p)$ is called the image of $s(t)$ under integral transform **F**.

The integral transforms are extremely useful in solving differential and difference equations. For example, one can often use the Laplace transform to reduce equations to simple algebraic expressions in the transform of the unknown function $s(t)$. At the same time, the initial or boundary conditions are automatically incorporated in the transform solution. This is in contrast with classical methods, in which the general solution must be fitted to these conditions. Solutions are often expedited through the use of tables and a small set of theorems about the characteristics of the transform. The transform method can also provide a great amount of intuition about the physical system being modeled.

In addition to their uses in solving and analyzing differential and differences equations, the transforms have found an application for solving certain classes of integral and integro-differential equations.

2.2.2 Integral transforms: definitions and relationships

The Fourier integral transform (direct and inverse) for the function $s(t)$ is defined on the whole time axis:

$$\mathbf{F}\{s(t)\} = \int_{-\infty}^{\infty} s(t)e^{-j\omega t}dt = S(\omega); \qquad \mathbf{F}^{-1}\{S(\omega)\} = \frac{1}{2\pi}\int_{-\infty}^{\infty} S(\omega)e^{j\omega t}d\omega = s(t). \tag{6}$$

For a function $s(t)$ defined for $0 \le t < \infty$, and for real constants K and a such that $|s(t)| \ge Ke^{at}$, its Laplace integral transform (direct and inverse) is denoted as $S(p)$ obtained by the following pairs of integrals:

$$\mathbf{L}\{s(t)\} = \int_{-\infty}^{\infty} s(t)\, e^{-pt} dt = S(p); \qquad \mathbf{L}^{-1}\{S(p)\} = \lim_{b\to\infty} \frac{1}{2\pi j} \int_{a-jb}^{a+jb} S(p)\, e^{pt} dp = s(t). \tag{7}$$

It should be noted that for most physically realized functions their Laplace integral transforms exist.

The *z*-transform is nothing else than the Laplace integral transform for discrete functions if we introduce the new variable $z = e^{pt}$. For the function $f(t) = f(n\Delta) = f_n$ with discretization step Δ the *z*-transform is given by:

$$\mathbf{Z}\{f_n\} = \sum_{n=-\infty}^{\infty} f_n z^{-n} = F(z); \qquad \mathbf{Z}^{-1}\{F(z)\} = \frac{1}{2\pi j} \oint z^{m-1} F(z)\, dz = f_m. \tag{8}$$

2.2.3 Some properties of Laplace transforms

To use Laplace integral transforms more efficiently we have to mention some of their properties, which will be used in the next sections. Interested readers could refer to reference or textbooks on advanced and applied mathematics, e.g., Ovchinnikov (2000), Hanna and Rowland (1990), and Churchill (1972).

(a) Linearity: The Laplace transform is a linear operator. This implies that for constants α and β:

$$\mathbf{L}\{\alpha s_1(t) + \beta s_2(t)\} = \alpha \mathbf{L}\{s_1(t)\} + \beta \mathbf{L}\{s_2(t)\}.$$

(b) Shifting property of the original: A shift of τ units on the time axis can be accomplished in the transform domain by multiplying the transform of the function with its origin at $t = 0$ by $e^{-\tau p}$. That is,

$$\mathbf{L}\{s(t-\tau)\} = e^{-\tau p} S(p).$$

(c) Variable transform: Let the function $s(t)$ be the original, and $S(p)$ its image. Then for constant $a \ne 0$:

$$\mathbf{L}\{s(at)\} = \frac{1}{a} S\left(\frac{p}{a}\right).$$

(d) Shifting property of the image: Let $S(p)$ be the image of the original $s(t)$, and α a complex number. Then $S(p+\alpha)$ is the image of the function $e^{-\alpha t} s(t)$, or:

$$\mathbf{L}\{e^{-\alpha t} s(t)\} = S(p+\alpha).$$

(e) Derivative of the image: Let $S(p)$ be the image of the original $s(t)$. Then

$$\mathbf{L}\{-ts(t)\} = \frac{dS(p)}{dp},$$

$$\mathbf{L}\{(-t)^n s(t)\} = \frac{d^n S(p)}{dp^n}.$$

(f) Derivative of the original: Let the function $s(t)$ have a continuous derivative at $t > 0$, and let $s'(t)$ be the original. Then

$$\mathbf{L}\left\{\frac{ds}{dt}\right\} = \mathbf{L}\{s'(t)\} = pS(p) - s(0),$$

$$\mathbf{L}\{s^{(n)}(t)\} = p^n S(p) - p^{n-1}s(0) - p^{n-2}s'(0) - p^{n-3}s''(0) - \Lambda - s^{(1)}(0).$$

In the case that the initial conditions are zero, we have:

$$\mathbf{L}\{s^{(n)}(t)\} = p^n S(p).$$

(g) Integration of the original: Let $s(t)$ be the original, and $S(p)$ its image. Then $\int_0^t s(u)du$ is also an original, and its image is $\frac{S(p)}{p}$, or

$$\mathbf{L}\left\{\int_0^t \Lambda \int_0^t s(u)(du)^n\right\} = \frac{1}{p^n} S(p).$$

(h) Integration of the image: Let $\mathbf{L}\{s(t)\} = S(p)$, $\frac{s(t)}{t}$ be the original, and the integral $\int_p^\infty S(z)dz$ converge. Then

$$\mathbf{L}\left\{\frac{s(t)}{t}\right\} = \int_p^\infty S(z)dz.$$

(i) Initial theorem: $\lim_{t\to 0} s(t) = \lim_{p\to\infty} pS(p)$.

(j) Final-value theorem: $\lim_{t\to\infty} s(t) = \lim_{p\to 0} pS(p)$.

(k) Convolution: $\mathbf{L}\{S_1(p)S_2(p)\} = \int_0^t s_1(u)s_2(t-u) \equiv s_1(t) * s_2(t)$.

(l) The first expansion theorem: $\mathbf{L}\left\{\frac{t^n}{n!}\right\} = \frac{1}{p^{n+1}}$.

(m) The second expansion theorem: If the image is a fractional rational function, i.e., the numerator and denominator are polynomials in p: $S(p)=\frac{F_q(p)}{G_n(p)}$, where the degree of numerator q is less than the degree of denominator n, moreover the denominator has zeros α_1, α_2, …, α_m of corresponding multiplicities k_1, k_2, …, k_m $(k_1+k_2+\Lambda+k_m=n)$, then the original for $S(p)$ can be determined by the expression:

$$s(t)=\sum_{i=1}^{m}\frac{1}{(k_i-1)!}\lim_{p\to\alpha_i}\frac{d^{k_i-1}}{dp^{k_i-1}}\left[(p-\alpha_i)^{k_i}\frac{F_q(p)}{G_n(p)}e^{pt}\right].$$

Consequence: If the denominator $G_n(p)$ has distinct zeros α_1, α_2, …, α_n, then we have the Heaviside expansion formula for the original:

$$s(t)=\sum_{i=1}^{n}e^{\alpha_i t}\frac{F_q(\alpha_i)}{G_n'(\alpha_i)}.$$

2.2.4 The nature of the p-domain

The Laplace integral transform, like all transforms, changes one signal into another according to a fixed set of rules (Smith, 1999). This transform sets up a univocal correspondence between a signal (called, original) in the time domain, and a signal (also called, image) in the *p*-domain. The original has to be a continuous function of time on the whole time axis. The *p*-domain is a complex plane. So, the abscissa axis corresponds to real numbers and variable σ, and the ordinate axis corresponds to imaginary numbers and variable ω. The location of any point on the *p*-plane can be represented by a pair of variables σ and ω, or alternatively by a single complex variable $p=\sigma+j\omega$, where j is the imaginary unit. Traditionally images by Laplace are represented by capital letters. For example, a time domain signal $s(t)$ is transformed into the *p*-domain signal $S(p)$, or alternatively $S(\sigma,\omega)$. The *p*-plane is continuous and extends to infinity in all four directions.

The image by Laplace is a function defined on the *p*-domain and takes on values that are also complex numbers. In other words, each point of the *p*-plane corresponds to the complex value of the image. As with all complex numbers, the real and imaginary parts of the image can alternatively be interpreted as the magnitude and the phase.

In the same way as the Fourier transform examines signals in terms of sinusoids, the Laplace transform examines signals in terms of sinusoids and exponentials. From a mathematical point of view, this makes the Fourier transform a subset of the more general Laplace transform. Figure 5 explains the strategy behind the Laplace integral transform. To find the values along a vertical line in the *p*-plane (the values at a fixed σ), the original is first multiplied by the exponential curve $e^{-\sigma t}$. The left half of the *p*-plane multiplies the original with exponentials that increase with time $(\sigma<0)$, while in

the right half the exponentials decrease with time $(\sigma > 0)$. Next, take the complex Fourier transform of the exponentially weighted signal. The resulting spectrum is placed along a vertical line in the *p*-plane, with the top half of the *p*-plane containing the positive frequencies and the bottom half containing the negative frequencies. The values on the ω-axis (ordinate axis) of the *p*-plane $(\sigma = 0)$ are exactly equal to the Fourier transform of the original signal.

Let us remember that the expression for Fourier transform in the complex form for signal $s(t)$ is given by:

$$S(\omega) = \int_{-\infty}^{\infty} s(t) e^{-j\omega t} dt \,. \tag{9}$$

This can be expanded into the Laplace transform by first multiplying the original signal by the exponential term:

$$S(\sigma, \omega) = \int_{-\infty}^{\infty} \left[s(t) e^{-\sigma t} \right] e^{-j\omega t} dt \,. \tag{10}$$

To place the equation in a shorter form, the two exponential terms can be combined:

$$S(\sigma, \omega) = \int_{-\infty}^{\infty} s(t) e^{-(\sigma + j\omega)t} dt \,. \tag{11}$$

And finally, the location in the complex plane can be represented by the complex variable p, where $p = \sigma + j\omega$. This allows equation (11) to be reduced to the more compact expression:

$$S(p) = \int_{-\infty}^{\infty} s(t) e^{-pt} dt \,. \tag{12}$$

STEP 1
Begin with the original $s(t)$.

STEP 2
Multiply the original by an infinite number of exponential curves, each with a different decay constant σ. That is, calculate the signal $s(t)e^{-\sigma t}$ for each value of σ from negative to positive infinity.

STEP 3
Take the complex Fourier Transform of each exponentially weighed original. That is, calculate

$$\int_{-\infty}^{\infty} \left[s(t)e^{-\sigma t} \right] e^{-j\omega t}\, dt$$

for each value of σ from negative to positive infinity.

STEP 4
Arrange each spectrum along a vertical line in the p-plane. The positive frequencies are in the upper half of the p-plane while the negative frequencies are in the lower half.

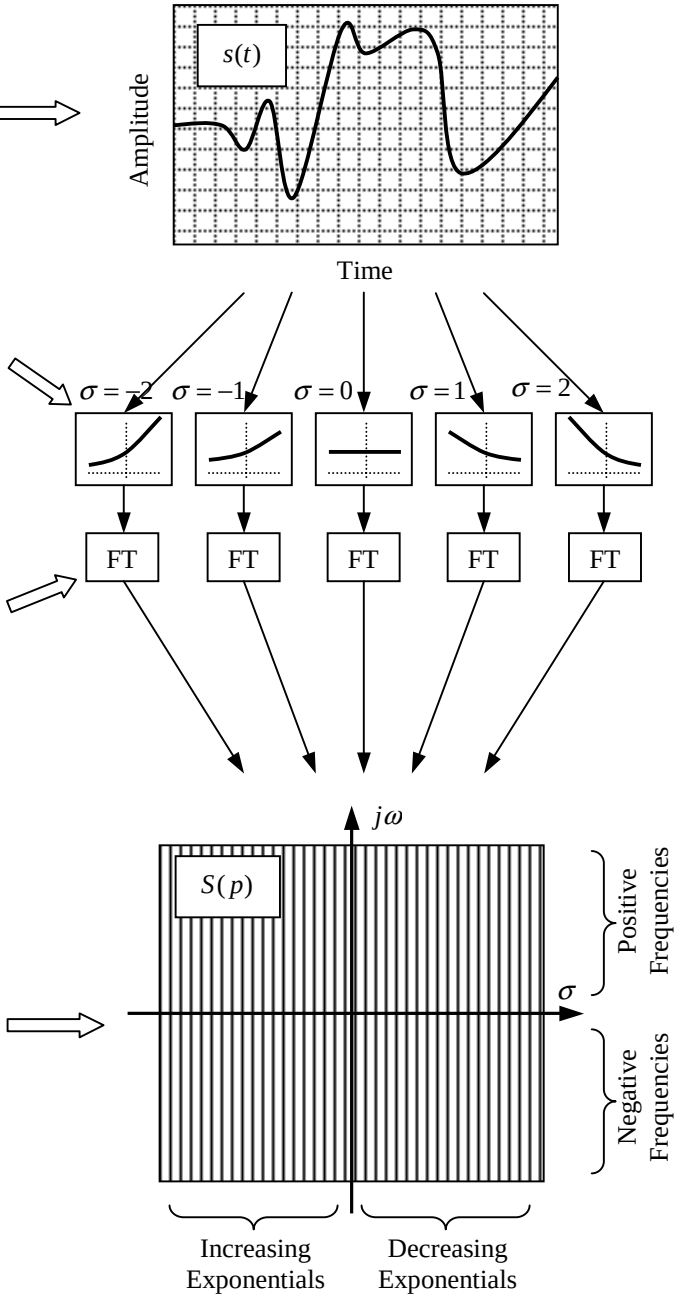

Figure 5: The strategy behind the Laplace integral transform (Smith, 1999). The Laplace integral transform converts a signal in the time domain $s(t)$ into a signal in the *p*-domain $S(p)$ or $S(\sigma, \omega)$. The values along each vertical line in the *p*-domain can be found by multiplying the time domain signal by an exponential curve with the decay constant σ, and taking the complex Fourier transform. When the time domain is entirely real, the upper half of the *p*-plane is a mirror image of the lower half.

2.3 Application of Laplace Integral Transform to Verification Time Calculations

2.3.1 VT calculations in the Laplace space

The condition for verification (1) is a difference inequality, so we can perform the analysis of the VT using Laplace integral transform.

Let the images in the Laplace space are $S(p)$ and $E(p)$, which correspond to the functions of the emission $s(t)$ and uncertainty $\varepsilon(t)$, respectively:

$$s(t) \leftrightarrow S(p); \qquad \varepsilon(t) \leftrightarrow E(p). \tag{13}$$

The VT concept in the time domain can be expressed as:

$$\left|s(t) - s(t-\tau)\right| \geq \varepsilon(t). \tag{14}$$

For verification time ascertainment we consider the equation that corresponds to inequality (14) in the space of images. After the transition into the image space and using the shifting property of the Laplace integral transform, we obtain:

$$\tau(p) = -\frac{1}{p}\ln\left(1 - \frac{E(p)}{S(p)}\right) \text{ for } s(t) \geq s(t-\tau) \text{ (increasing emission signal);} \tag{15}$$

$$\tau(p) = -\frac{1}{p}\ln\left(1 + \frac{E(p)}{S(p)}\right) \text{ for } s(t) < s(t-\tau) \text{ (decreasing emission signal).} \tag{16}$$

Thus, the verifiability of a GHG emitting system is related to the ratio of images of the emission signal and uncertainty, respectively, in the *p*-domain. This ratio has to be interpreted not only as their magnitude fraction; it also reflects the so-called phase correlation between the emission signal and its uncertainty.

We have obtained the expressions (15) and (16) for the verification time τ as functions of the model variable p. To obtain the expression for τ in the time domain, we need to carry out the inverse Laplace transform of $\tau(p)$ according to definition (7); or, if the expressions (15) or (16) are sufficiently simple, we can try to use a table of Laplace transforms of known functions in combination with given transform properties. In the event that these means are impracticable, one can always use numerical methods for finding the inverse Laplace transform (Duffy, 1993).

2.3.2 Determining behavior of the function of the emission signal

With help of the Laplace integral transform of the inequality for the VT [equation (1)], one can determine properties of the function describing the emission signal defined by its verification time τ.

Let us consider the case of a decreasing signal:

$$s^*(t) - s^*(t+\tau) = \varepsilon(t). \tag{17}$$

By implementing the Laplace integral transform we obtain:

$$S^*(p) = \frac{E(p)}{1-e^{-qp}}, \tag{18}$$

where $S^*(p)$ is the Laplace image of the limit function $s^*(t)$ of the emission signal $s(t)$, $E(p)$ is the Laplace image of the uncertainty $\varepsilon(t)$, p is the model variable, and τ is the verification time. To obtain the original for $S(p)$, one has to apply the inverse Laplace integral transform to the image $S(p)$. Thus, to satisfy the verification condition (1), the emission signal $s(t)$ has to decrease identically or faster than the limit function $s^*(t)$ between t_1 and t_2.

2.3.3 Dynamical signal representation

To represent the emission signal and its uncertainty with the help of the Laplace integral transform, the real structure of the existent data has to be considered. Such data are available as mean annual emissions and their uncertainties. Thus, the real emission signal (as well as its uncertainty) can be approximated by the sum of elementary signals (with a time step of $\Delta = 1$ year). There are two formal possibilities for such representation:

(i) the dynamical representation of the emission signal with the help of Heaviside's function $\sigma(t)$, and

(ii) the dynamical representation of the emission signal with the help of Dirac's delta-function $\delta(t)$.

The first method corresponds to Figure 6a, where multi-step functions are used as elementary signals that appear in equal time intervals Δ. In the second method (Figure 6b), rectangular pulses serve as elementary signals that follow one another in equal time intervals Δ.

The first case of dynamical signal representation is realized by:

$$s(t) = s(0)\sigma(t) + \int_0^\infty \frac{ds}{d\tau}\sigma(t-\tau)d\tau, \tag{19}$$

where Heaviside's function $\sigma(t)$ is defined as:

$$\sigma(t) = \begin{cases} 0, & t < 0, \\ 1, & t \geq 0. \end{cases} \tag{20}$$

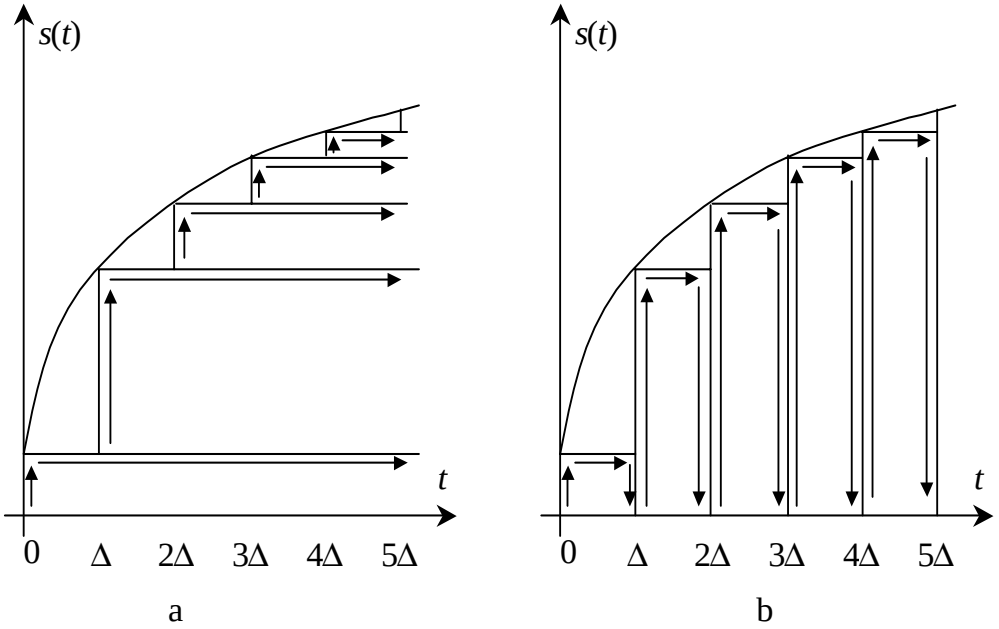

Figure 6: Dynamical signal representation. The first case corresponds to the representation where multi-step functions are used as elementary signals that appear in equal time intervals Δ. In the second method, rectangular pulses serve as elementary signals that follow one another in equal time intervals Δ.

The second case is realized by:

$$s(t) = \int_{-\infty}^{\infty} s(\tau)\delta(t-\tau)d\tau, \tag{21}$$

where $\delta(t)$ is Dirac's delta-function. In the theory of generalized functions there are many ways to define the Dirac's delta-function by functional sequences (Churchill, 1972; Hanna and Rowland, 1990); here we use the following one:

$$\delta(t) = \begin{cases} \infty, & t = 0, \\ 0, & t \neq 0, \end{cases} \text{ and } \int_{-\infty}^{\infty} \delta(t)dt = 1. \tag{22}$$

We will consider the representation of the emission signal where the multi-step functions are used as elementary signals that appear in equal time intervals Δ (the first case):

$$\begin{aligned} &s(t) = s_0\sigma(t) + (s_1 - s_0)\sigma(t-\Delta) + (s_2 - s_1)\sigma(t-2\Delta) + \Lambda = \\ &= s_0\sigma(t) + \sum_{k=1}^{\infty}(s_k - s_{k-1})\sigma(t-k\Delta) = \sum_{k=0}^{\infty} s_k\left[\sigma(t-k\Delta) - \sigma(t-k\Delta-\Delta)\right], \end{aligned} \tag{23}$$

where s_k are signal values at points in time, $t_k = k\Delta$, $(k = \overline{0,\infty})$.

Taking into consideration that $L\{\sigma(t)\}=\frac{1}{p}$, and using the shifting property of the image (property (d), see Section 2.2.3), we obtain the Laplace image of the signal represented by equation (23):

$$S(p)=\frac{1-e^{-p\Delta}}{p}\sum_{k=-\infty}^{\infty}s_k e^{-pt_k}\ , \tag{24}$$

where Δ is the discretization time interval (typically 1 year), and s_k reflects the annual emissions for *k*-th year.

3 Analysis of Applying the Laplace Integral Transform to the VT Concept and Identifying the Potentials of Different Systems Emitting Greenhouse Gases

3.1 Sensitivity Analysis of Signal Representation by Laplace

In reality, considerable uncertainty underlies the emission data. In many cases this uncertainty may be comparable to the order of emission levels. Additionally, very often the emission data are described by polynomial functions in time, where the polynomial coefficients play the role of dynamical moments of the emission signal (mean value, velocity, acceleration, and dynamical moments of higher orders). In light of the aforementioned uncertainties, the question of how sensitive the Laplace integral representation of such a signal to variations in its polynomial coefficients is interesting. To these ends, we will look into how one Laplace signal representation differs from another representation of the same signal, if the polynomial coefficients that represent the emission signal in the time domain are permitted to vary.

To begin with, we will consider the question of how sensitive the signal representation by a polynomial function in the time domain is to uncertainties in the polynomial coefficients. Let the emission signal be described by a polynomial function of the order n:

$$s(t)=\sum_{k=0}^{n}\frac{s_k}{k!}t^k\ . \tag{25}$$

Using the first expansion theorem (property (l), see Section 2.2.3) we take Laplace transform of the signal represented by equation (25). Then, the Laplace image of the signal will also be described by a polynomial but with the negative exponents with respect to the Laplace variable p:

$$S(p)=\sum_{k=0}^{n}\frac{s_k}{p^{k+1}}\ . \tag{26}$$

Let us consider the variation $\delta s(t)$ of the original signal $s(t)$ induced by a variation δs_i of the polynomial coefficient s_i ($0 \le i \le n$):

$$\delta s(t) = \frac{\delta s_i}{i!} t^i, \tag{27}$$

which is inverse proportional to $i!$, the order of the signal dynamical moment under discussion, and proportional to t^i, the time interval for which the signal is represented by the polynomial. That is, for a given time interval less accuracy is needed for higher polynomial coefficients.

Similarly, we consider the variation $\delta S(p)$ of the signal image $S(p)$ induced by a variation δs_i of the polynomial coefficient s_i ($0 \le i \le n$):

$$\delta S(p) = \frac{\delta s_i}{p^{i+1}}. \tag{28}$$

The variation $\delta S(p)$ has the same significance value as variation $\delta s(t)$ in equation (27); this significance decreases with increasing the number i. So, the higher accuracy of the coefficient s_i is necessary to represent lower "spectral" components of the signal in the space of originals.

As a measure to evaluate the quality of representing one signal by another of the emission signal and uncertainty, it is proposed to use the norm of the signal (uncertainty) that reflects its energy E, and distance between two signals as a norm of their difference:

$$\|s(t)\| = \sqrt{\int_0^\infty s^2(t)dt} = \sqrt{E}, \tag{29}$$

where $\|s(t)\|$ is the norm of the signal. Then $\|s_1 - s_2\| = \sqrt{\int_0^\infty (s_1(t) - s_2(t))^2 dt}$ is the distance between the signals $s_1(t)$ and $s_2(t)$.

3.2 Analysis of VT Depending on the Dynamics of Uncertainties

Since we have obtained expressions (15) and (16) for the verification time in an explicit form in the *p*-domain, the question arises of how the verification time depends on the change in uncertainty. To these ends, it is proposed for the time being to accept $E(p)$ as an independent variable in equations (15) and (16), i.e., we consider the derivative of the verification time with regard to $E(p)$ in these equations. In the case of an increasing emission signal (15), we have:

$$\frac{d\tau}{dE} = \frac{1}{S(p) - E(p)} = \frac{e^{p\tau}}{S(p)}, \tag{30}$$

where the difference $S(p) - E(p)$ is replaced by $S(p)e^{-p\tau}$ from equation (15).

Now we can introduce the sensitivity parameter β as a measure of change in verification time due to a 1% change in uncertainty. It is defined in the *p*-domain by:

$$\beta = \frac{E(p)}{100}\frac{d\tau}{dE}. \tag{31}$$

Taking into account expression (30), we find:

$$\beta = \frac{1}{100}\frac{E(p)}{S(p) - E(p)} = \frac{1}{100}\frac{E(p)}{S(p)}e^{p\tau}. \tag{32}$$

It should be noted that introducing the sensitivity parameter β in the *p*-domain is purely formal. As a matter of fact, the physical meaning of β in the *p*-domain is lost. This is because equation (32) is valid in the *p*-domain for images $E(p)$ and $S(p)$, which take on complex values (it is impossible to say which complex number is bigger and by how much). To obtain an expression for β in the time domain, we need to transform equation (32) into the space of originals according to definition (7) or use a table of Laplace transform and its properties. In the event that these means are impracticable, one can use numerical methods for finding the inverse Laplace transform, e.g., presented in Duffy (1993).

If we introduce a similar parameter α, which expresses the sensitivity of the VT due to a change in the emission signal, then $\alpha = -\beta$. So, from the point of view of verification in the image space, there is not a difference in the sensitivity of the emission signal and its uncertainty.

3.3 Determining Parameters of the Systems Emitting Greenhouse Gases

A convenient mathematical apparatus for modeling dynamical systems are differential equations. The Laplace integral transform is a natural tool for solving them. In the case of a system of linear differential equations one can apply the Laplace transform to the system and change it into simple algebraic expressions of the unknown function.

In this section, it is proposed to investigate GHG emitting systems, under the assumption that their dynamics can be modeled by a system of linear differential equations. Time intervals are assumed to be sufficiently small so that the coefficients in the equations are constant.

Let the following system of differential equations of dimension n describes the system investigated:

$$\begin{cases} \dfrac{ds_1}{dt} = a_{11}s_1(t) + a_{12}s_2(t) + \cdots + a_{1n}s_n(t) + g_1(t), \\ \dfrac{ds_2}{dt} = a_{21}s_1(t) + a_{22}s_2(t) + \cdots + a_{2n}s_n(t) + g_2(t), \\ \vdots \\ \dfrac{ds_n}{dt} = a_{n1}s_1(t) + a_{n2}s_2(t) + \cdots + a_{nn}s_n(t) + g_n(t), \end{cases} \tag{33}$$

where for $i = \overline{1,n}$ and $j = \overline{1,n}$ $s_i(t)$ are state variables (describing the emissions of the *i*-th box of the system); a_{ij} is a constant coefficient (describing the rate of emission flow from the *j*-th box to the *i*-th box); g_i is an external disturbance of the system (describing the external force or activity performed in the *i*-th box).

As is well known from the theory of differential equations, the general solution of system (33) in the case of real or complex roots of characteristic equation of the corresponding homogeneous system can be expressed by:

$$s_i(t) = \sum_{j=1}^{n} \gamma_{ij} c_j(t) e^{\lambda_j t} + s_i^*(t), \; i = \overline{1,n}; \tag{34}$$

where λ_j are the roots (real or complex) of the characteristic equation of the corresponding homogeneous system; n is the order of the system; $c_j(t)$ are coefficients (functions in t or constants); γ_{ij} are the components of the characteristic vectors corresponding to the λ_j; and $s_i^*(t)$ is the partial solution of the non-homogeneous system of differential equation (Ovchinnikov, 2000; Birkhoff and Rota, 1978). In the case of an undisturbed system, when $g_i(t) \equiv 0$ $(i = \overline{1,n})$, the solution of system (33) is:

$$s_i(t) = \sum_{j=1}^{n} \gamma_{ij} c_j e^{\lambda_j t}, \; i = \overline{1,n}; \tag{35}$$

where c_j are constants defined by the initial conditions for system (33).

Let us consider the Laplace transform for expression (35). Using the linearity of the Laplace transform (property (a) in the Section 2.2.3) and taking into account that $\mathbf{L}\{e^{\lambda t}\} = \dfrac{1}{p-\lambda}$, we obtain:

$$S_i(p) = \sum_{j=1}^{n} \frac{\gamma_{ij} c_j}{p - \lambda_j}, \; i = \overline{1,n}. \tag{36}$$

Expression (36) allows us to determine the roots of the characteristic equation of the corresponding homogeneous system λ_j from it (the $S(p)$ approaches infinity when p approaches λ_j).

Let us assume that we face the difficulties of constructing a system of equations like (33) because of the overly great dimension of the system to be modeled or lack of data that are necessary for setting up such a system of equations. Let us additionally assume that we have the dynamical data defining the state of some boxes (even one of them) of the system to be modeled (signal $s_i(t)$). Then, performing the Laplace transform of such a signal, we can calculate some or more of the λ_j (depending on the representability of the signal $s_i(t)$ investigated). These λ_j are the parameters of the system modelled, and they define to a certain extent an inner structure of the undisturbed system.

Thus, it appears that the task of determining the characteristic numbers for our GHG emitting system is equivalent to the task of reducing the emission signal to the form of equation (36) and investigating the latter with respect to its poles.

In a simple case (when the signal in equation (35) can be represented by an exponential function) these characteristic numbers correspond to exponential growth (decay) constants.

3.4 Detecting Specific Features for Systems Emitting GHGs

As explained in Section 2.3.3, the real emission signal (uncertainty) can be approximately realized by the sum of elementary signals (rectangular impulses) that appear in the time domain with a time step of one year.

Figure 7 shows an example of a rectangular pulse in the time domain, its frequency spectrum, and its *p*-domain representation (Smith, 1999). The rectangular pulse has a width of two and a height of one. Taking into account that $L\{\sigma(t)\}=\frac{1}{p}$ (see Section 2.3.3) and using shifting property (b) of the Laplace transform (see Section 2.2.3), we evaluate the corresponding *p*-domain signal, expressed in terms of the complex location p, and the complex value $S(p)$:

$$S(p)=\frac{e^{p}-e^{-p}}{p}. \tag{37}$$

The topographical surfaces in Figure 7 are graphs of the equation (37), where the complex variable p is decomposed in its real and imaginary part.

In our case (GHG emitting systems) the signal consists of a sum of elementary rectangular pulses shifted in time. Such a signal corresponds to the superposition of the images like (37) and presented in Figure 7. As a result, we obtain the “spectral” portrait

of the signal investigated in the *p*-domain, which can help one detect specific features for different signals and thus for different systems emitting GHGs. This is a probable way of predicting the future dynamics of systems by investigating their past dynamics.

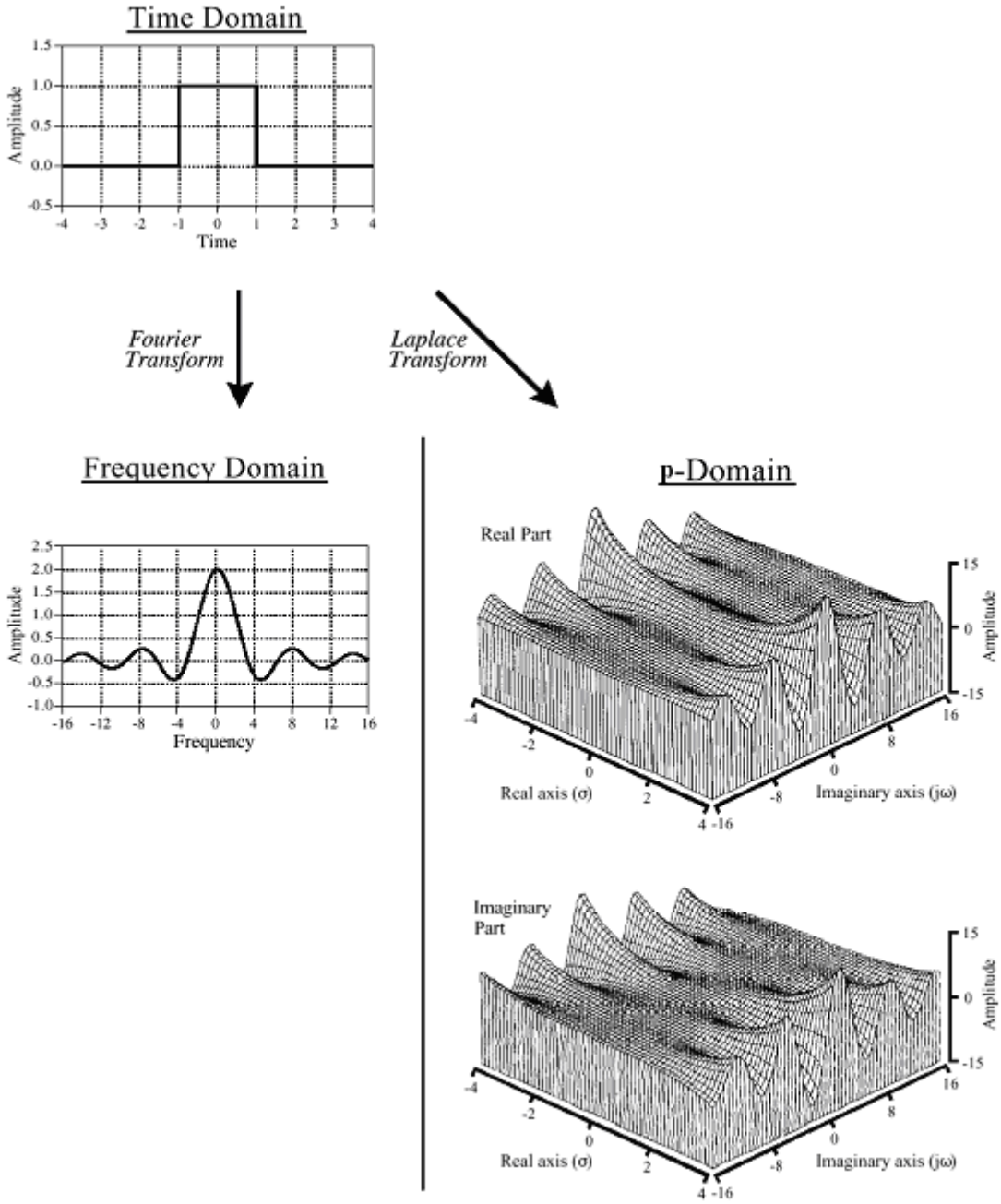

Figure 7: Time, frequency and *p*-domain. A time domain signal (the rectangular pulse) is transformed into the frequency domain using the Fourier transform, and into the *p*-domain using the Laplace transform (Smith, 1999).

4 Conclusions

The main task of this study is to investigate the usefulness of the Laplace integral transform for verifying emission signals of GHG emitting systems. Particular conclusions arise from this study:

- The verifiability of GHG emitting systems is related to the ratio of the images of the emission signal and uncertainty (equations (15) and (16) in Section 2.3.1). In the Laplace domain, this ratio reflects not only the amplitude ratio of the signal to uncertainty, but also their so-called phase correlation;
- The emission signal can be described as a sum of elementary signals (rectangular pulses) in the time domain with a time step of one year, which is sufficient to process and represent real emission data and their uncertainties;
- If the emission signal is presented by a polynomial function in time *t*, then its L-image is also presented by a polynomial function in the Laplace variable *p* with negative exponents. Therefore, coefficients of *p*-terms with smaller exponents need to be defined more precisely;
- The Laplace integral transform allows modeling GHG emitting systems by the systems of differential equations and determining the characteristic numbers for the GHG emitting system, which serve as parameters of the system modeled and define, to a certain extent, an inner structure of the system;
- With the help of "spectral" emission portraits in the Laplace domain, it is hoped that one can detect specific features of the signals. This may permit the prediction of possible system behaviors, and thus to link a signal's past dynamics with its future dynamics.

The application of integral transforms appears promising to discover the dynamics of different GHG emitting systems. This problem is of great interest and demands a better understanding of the features and potentials of these systems.

References

Birkhoff, G. and G. Rota (1978). *Ordinary Differential Equations*. Third edition. Wiley, New York, USA.

Churchill, R. (1972). *Operational Mathematics*. Third edition. McGraw-Hill, New York, USA.

Duffy, D.G. (1993). On the Numerical Inversion of Laplace Transforms: Comparison of Three New Methods on Characteristic Problems From Applications. *ACM Transactions on Mathematical Software*, Vol. 19, No. 3, 333–359. Available on the Internet: http://www.acm.org/pubs/citations/journals/toms/1993-19-3/p333-duffy/.

Gusti, M. and W. Jęda (2002). Carbon Management: A New Dimension of Future Carbon Research. Interim Report IR-02-006. International Institute for Applied Systems Analysis, Laxenburg, Austria.

Hanna, J.R. and J.H. Rowland (1990). *Fourier Series, Transforms, and Boundary Value Problems*. Second Edition. Wiley, New York, USA.

IPCC (2000). Good Practice Guidance and Uncertainty Management in National Greenhouse Gas Inventories. Intergovernmental Panel on Climate Change (IPCC). Available on the Internet: http://www.ipcc-nggip.iges.or.jp/gp/report.htm.

IPCC/OECD/IEA (1997). Expert Group Meeting on Methods for the Assessment of Inventory Quality. IPCC/OECD/IEA Program on National Greenhouse Gas Inventories. Report of the Meeting held on 5–7 November 1997, Bilthoven, Netherlands. Available on the Internet: http://www.ipcc-nggip.iges.or.jp/public/mtdocs/tdbusm.htm.

Jonas, M. and S. Nilsson (2001). The Austrian Carbon Database (ACDb) Study — Overview. Interim Report IR-01-064. International Institute for Applied Systems Analysis, Laxenburg, Austria.

Jonas, M., S. Nilsson, A. Shvidenko, V. Stolbovoi, M. Gluck, M. Obersteiner and A. Öskog (1999a). Full Carbon Accounting and the Kyoto Protocol: A Systems-Analytical View. Interim Report IR-99-025. International Institute for Applied Systems Analysis, Laxenburg, Austria.

Jonas, M., S. Nilsson, M. Obersteiner, M. Gluck, and Y. Ermoliev (1999b). Verification Times Underlying the Kyoto Protocol: Global Benchmark Calculations. Interim Report IR-99-062. International Institute for Applied Systems Analysis, Laxenburg, Austria.

Jonas, M., M. Obersteiner and S. Nilsson (2000). How to Go From Today's Kyoto Protocol to a Post-Kyoto Future that Adheres to the Principles of Full Carbon Accounting and Global-scale Verification? Interim Report IR-00-061. International Institute for Applied Systems Analysis, Laxenburg, Austria.

Marland, G., T.A. Boden, R.J. Andres, A.L. Brenkert and C. Johnston (1999). Global, Regional, and National CO_2 Emissions. In: *Trends: A Compendium of Data on Global Change*. Carbon Dioxide Information Analysis Center, Oak Ridge National Laboratory, US Department of Energy, Oak Ridge, Tennessee, USA. The database is available in the Internet: http://cdiac.esd.ornl.gov/ndps/ndp030.html.

Nilsson, S., A. Shvidenko, V. Stolbovoi, M. Gluck, M. Jonas and M. Obersteiner (2000). Full Carbon Accounting for Russia. Interim Report IR-00-021. International Institute for Applied Systems Analysis, Laxenburg, Austria.

Obersteiner, M., Y. Ermoliev, M. Gluck, M. Jonas, S. Nilsson and A. Shvidenko (2000a). Avoiding a Lemons Market by Including Uncertainty in the Kyoto Protocol: Same Mechanism — Improved Rules. Interim Report IR-00-043. International Institute for Applied Systems Analysis, Laxenburg, Austria.

Obersteiner, M., M. Jonas and S. Nilsson (2000b). The Political and Economic Costs of a Fully Verifiable Kyoto Protocol. Interim Report IR-00-062. International Institute for Applied Systems Analysis, Laxenburg, Austria

Obersteiner, M., M. Jonas, S. Nilsson, A. Shvidenko and M. Gluck (2000c). If You Act Locally and Compute Globally: What is the Optimal Comprehensiveness of the Reference Carbon System? Interim Report IR-00-065. International Institute for Applied Systems Analysis, Laxenburg, Austria

Ovchinnikov, P. (2000). *Advanced Mathematics*. In Two Parts. Second edition. Tekhnika, Kyiv, Ukraine (in Ukrainian).

Smith, S.W. (1999). *The Scientist and Engineer's Guide to Digital Signal Processing*. California Technical Publishing, San Diego, California, USA.

UNFCCC (1998). Report of the Conference of the Parties on Its Third Session, Held at Kyoto From 1 to 11 December 1997. United Nations Framework Convention on Climate Change (UNFCCC). Addendum. Document FCCC/CP/1997/7/Add.1. Available on the Internet: http://www.unfccc.de/.

UNFCCC (2000). Searchable Greenhouse Gas Inventory Database. United Nations Framework Convention on Climate Change (UNFCCC). Available on the Internet: http://www.unfccc.de/.